Manuscript Number:

Title: Calculation of nanoparticle capture efficiency in magnetic drug targeting

Article Type: Regular Submission

Corresponding Author: Dr Patrick Joseph Cregg, PhD

Corresponding Author's Institution: Waterford Institute of Technology

First Author: Patrick Joseph Cregg, PhD

Order of Authors: Patrick Joseph Cregg, PhD; Kieran Murphy, PhD; Adil Mardinoglu, BEng

Abstract: The magnetic targeted drug delivery system of Avil´es, Ebner and Ritter, which uses high gradient magnetic separation (HGMS) is considered. In that model large ferromagnetic particles are used as seeds to aid collection of multiple domain nanoparticles (radius ≈ 200 nm). Here, in contrast, single domain magnetic nanoparticles (radius in 20-100 nm) are considered and the Langevin function is used to describe the magnetization. Simulations based on this model were performed using the open source C++ finite volume library OpenFOAM. The simulations indicate that use of the Langevin function predicts greater collection efficiency than might be otherwise expected.

Cover Letter

Dr PJ Cregg
Materials Characterisation & Processing Group
Waterford Institute of Technology
Waterford
Ireland
pjcregg@wit.ie
tel ++353 51 302631
mobile ++353 87 6798710

Dear Prof Chantrell,

Please find attached a copy of *Calculation of nanoparticle capture efficiency in magnetic drug targeting* by P.J. Cregg , Kieran Murphy, Adil Mardinoglu which I hope will be of interest to readers of the *Journal of Magnetism and Magnetic Materials.*

Best regards
 Dr P J Cregg

Calculation of nanoparticle capture efficiency in magnetic drug targeting

P.J. Cregg *, Kieran Murphy, Adil Mardinoglu

Materials Characterisation and Processing Group, Waterford Institute of Technology, Waterford, Ireland

Abstract

The magnetic targeted drug delivery system of Avilés, Ebner and Ritter, which uses high gradient magnetic separation (HGMS) is considered. In that model large ferromagnetic particles are used as seeds to aid collection of multiple domain nanoparticles (radius $\approx 200\,\text{nm}$). Here, in contrast, single domain magnetic nanoparticles (radius in 20–100 nm) are considered and the Langevin function is used to describe the magnetization. Simulations based on this model were performed using the open source C++ finite volume library OpenFOAM. The simulations indicate that use of the Langevin function predicts greater collection efficiency than might be otherwise expected.

Key words: magnetic drug targeting, high gradient magnetic separation (HGMS), magnetic nanoparticles, simulation, magnetic seed

PACS: 47.63.mh, 47.63.-b, 87.85.gf

* Corresponding author.
Email address: `pjcregg@wit.ie` (P.J. Cregg).

1 Introduction

Magnetic nanoparticles continue to offer much promise as carriers in drug targeting systems [1, 2]. That the force exerted on an individual particle is determined by the gradient of the field and not simply the field is well known [1, 3–8]. As has been pointed out by several authors [3–8] this may inhibit the targeting, solely by means of external permanent magnets, of areas deep within the body. With this in mind, the implanting of ferromagnetic materials, such as wires, seeds or stents, in blood vessels has been proposed by some authors [4–7], in order to create large localised gradients within the vessels. Berry [2] has suggested that magnetic nanoparticles with radius of the order of $50\,\mathrm{nm}$ may have advantages as drug carriers, and here these are taken as the carriers. For a related problem, Furlani and Furlani [9] have developed a model for which it was possible to obtain an analytical expression for the behaviour of multifunctional particles. In contrast, the approach taken here is largely numerical in that while the magnetic field is obtained from an analytical expression both the fluid flow and resulting particle trajectories are obtain using OpenFOAM a finite volume simulation C++ library.

2 Outline of Model

The model of Avilés, Ebner and Ritter [10], is considered, which uses ferromagnetic material, to create a localised field gradient, at the desired site in the body. This ferromagnetic material, termed seed, has a radius of the order of $1\,\mu\mathrm{m}$. The model treats the behaviour of magnetic particles under the
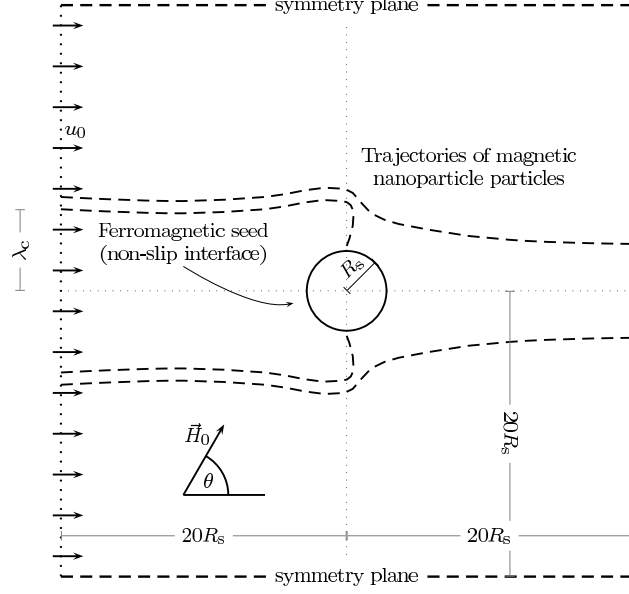
2

Fig. 1. Schematic diagram of the control volume, CV, used in determining the capture radius, λ_{c}, of the superparamagnetic single-domain nanoparticles.

41 influence of Stokes drag and the magnetic force. The Stokes drag is given by

$$\vec{F}_{\mathrm{s}} = 6\pi\,\eta_{\mathrm{b}}\,R_{\mathrm{p}}\,(\vec{v}_{\mathrm{b}} - \vec{v}_{\mathrm{p}}), \tag{1}$$

42 where η_{b} is the viscosity of the blood, R_{p} the radius of the particle, and $\vec{v}_{\mathrm{b}}$

43 and $\vec{v}_{\mathrm{p}}$ are the velocities of the blood and the particle respectively. The blood

44 velocity, $\vec{v}_{\mathrm{b}}$, is determined by solving the appropriate Navier-Stokes equations.

45 The magnetic force is determined by

$$\vec{F}_{\mathrm{m}} = (\vec{m} \cdot \nabla)\,\vec{B}, \tag{2}$$

46 where $\vec{B}$ is the resulting magnetic flux density (due to the external magnetic

47 field $\vec{H}$ and the presence of the seed) and $\vec{m}$ is the magnetic moment of the

48 particle. We follow Avilés *et al.* [10] and consider the effect of a magnetisable

49 seed placed in the blood flow as indicated in Fig. 1. The magnetisation of the

50 seed can be calculated from

$$M_{\mathrm{seed}} = 2\alpha_{\mathrm{seed}}H_0, \tag{3}$$

3

where α_{seed} is the demagnetising factor for an infinitely long cylinder in a perpendicular field taken as

$$\alpha_{\text{seed}} = \min\left(\frac{\chi_{\text{seed},0}}{2 + \chi_{\text{seed},0}}, \frac{M_{\text{seed,s}}}{2H_0}\right), \tag{4}$$

where $\chi_{\text{seed},0}$ and $M_{\text{seed,s}}$ are the zero field susceptibility and saturation magnetisation of the ferromagnetic seed respectively, and H_0 is the magnitude of the externally applied homogeneous field. In the model of Avilés et $al.$ microparticles were considered, where the axis of the moment $\vec{m}$ lay along that of $\vec{B}$, and the magnetisation increased with applied field, after accounting for demagnetising. In contrast, nanoparticles of diameter $< 100\,\text{nm}$ are typically superparamagnetic single domains. Accounting for thermal agitation, their average magnetisation is given by the Langevin function [3, 8, 11, 12]

$$L\left(\beta\right) = \coth\left(\beta\right) - \frac{1}{\beta}, \tag{5}$$

with Langevin argument

$$\beta = \frac{\mu_0\,\omega_{\text{fm,p}}\,V_{\text{p}}\,M_{\text{fm,p,s}}\,H}{kT}, \tag{6}$$

where μ_0 is the magnetic permeability of free space, $\omega_{\text{fm,p}}$ is the volume fraction of ferromagnetic material in the particle, V_{p} is the particle volume, $M_{\text{fm,p,s}}$ the (volume) saturation magnetisation, k is Boltzmann's constant and T is the absolute temperature, so that $\vec{m}$ can be written as

$$\vec{m} = \omega_{\text{fm,p}}\,V_{\text{p}}\,M_{\text{fm,p,s}}\,L\left(\beta\right)\frac{\vec{B}}{|\vec{B}|}. \tag{7}$$

The value of $\vec{B}$, required to calculate the magnetic force as given by Eqs. (2) and (7), is calculated from solving the Laplace equation as outlined in Section 4.

4

3 Blood flow — the Navier-Stokes equations

Following the notation of Avilés *et al.* [10] we write the blood velocity $\vec{v}_b$ and the pressure P for a incompressible, Newtonian fluid at steady state. We have the continuity equation

$$\nabla \cdot \vec{v}_b = 0, \tag{8}$$

and the Navier-Stokes equation

$$\rho_b[(\vec{v}_b \cdot \nabla \vec{v}_b)] = \nabla P + \eta_b \nabla^2 \vec{v}_b, \tag{9}$$

where ρ_b is the density of the blood. To solve Eqs. (8) and (9), a uniform inlet velocity profile is assumed at the inlet control volume (CV) such that

$$\vec{v}_b = \begin{pmatrix} u_0 \\ \\ 0 \end{pmatrix}, \tag{10}$$

where u_0 is the inlet blood velocity. Non-slip boundary conditions are applied at the seed surface in contact with the bloodstream. In addition, symmetry boundary conditions are applied at the upper and lower CV boundaries to maintain the constant flow profile and atmospheric pressure is assumed at the outlet of the CV to satisfy the boundary condition on pressure. Other assumptions include isothermal, single-phase, incompressible, Newtonian fluid flow as used by Avilés *et al.* [10].

4 The magnetic force — the scalar magnetic potential

The second part of this model involves the scalar magnetic potential, ϕ, which satisfies the Laplace equation over two con-joined regions: inside the seed and

outside the seed. From the scalar potential, we can obtain the magnetic flux density, $\vec{B}$, as required, through

$$\vec{B} = -\mu_0 \nabla \phi. \tag{11}$$

Thus for the two regions, within the seed and the rest of the space we have respectively $\vec{B}_{\mathrm{seed}}$ and $\vec{B}_{\mathrm{space}}$ as

$$\vec{B}_{\mathrm{seed}} = -\mu_0 (\vec{m}_{\mathrm{seed}} + \vec{H}_0 - \nabla \phi_{\mathrm{seed}}), \tag{12}$$

$$\vec{B}_{\mathrm{space}} = -\mu_0 (\vec{H}_0 - \nabla \phi_{\mathrm{space}}), \tag{13}$$

where ϕ_{seed} and ϕ_{space} represent the scalar magnetic potential within the seed and in the space outside the seed respectively. Here $\vec{m}_{\mathrm{seed}}$ is the induced magnetisation of the seed and $\vec{H}_0$ is the applied homogenous magnetic field given by

$$\vec{H}_0 = \begin{pmatrix} H_0 \cos \theta \\ H_0 \sin \theta \end{pmatrix}, \tag{14}$$

where θ is the angle from the positive x-axis. Laplace's equation for the scalar potential is solved analytically by separation of variables. Firstly, the normal component of the magnetic flux and potential are both assumed to be continuous across the seed-blood interface. Secondly, the scalar potential should tend towards zero far away from the seed. The required analytical solution is

$$\phi_{\mathrm{seed}} = H_0 \frac{\mu_{\mathrm{r}} - 1}{\mu_{\mathrm{r}} + 1}(x \cos \theta + y \sin \theta), \quad \phi_{\mathrm{space}} = H_0 \frac{\mu_{\mathrm{r}} - 1}{\mu_{\mathrm{r}} + 1} \frac{x \cos \theta + y \sin \theta}{x^2 + y^2}, \tag{15}$$

where μ_{r} is the relative permeability of the ferromagnetic seeds.

5   Velocity equations, streamlines and capture cross section

Considering the forces, the velocity equations can be obtained through com-
bining the hydrodynamic and magnetic velocities [10],

$$\vec{v}_\text{p} = \vec{v}_\text{b} + \frac{1}{2}V_\text{m}\frac{R_\text{seed}}{M_\text{seed,s}H_\text{f}}\nabla(\vec{H}_\text{f}\cdot\vec{H}_\text{f}), \tag{16}$$

where R_seed is the seed radius and $\vec{H}_\text{f}$ is the total magnetic field at the location
of the magnetic drug carrier particle and is given by

$$\vec{H}_\text{f} = \vec{H}_0 - \nabla\phi_\text{space}. \tag{17}$$

Here the magnitude of the total magnetic field H_f is given by $\sqrt{\vec{H}_\text{f}\cdot\vec{H}_\text{f}}$ so that

$$H_\text{f} = \sqrt{\left(H_0\cos\theta - \frac{\partial\phi_\text{space}}{\partial x}\right)^2 + \left(H_0\sin\theta - \frac{\partial\phi_\text{space}}{\partial y}\right)^2}. \tag{18}$$

The magnetic velocity, $\vec{v}_\text{m}$, is given by

$$\vec{v}_\text{m} = \frac{2}{9}\frac{R_\text{p}^2}{R_\text{seed}}\frac{\mu_0}{\eta_\text{b}}\omega_\text{fm,p}M_\text{seed,s}M_\text{fm,p,s}L(\beta). \tag{19}$$

The volume fraction of ferromagnetic material $\omega_\text{fm,p}$ in the magnetic drug
carrier particle is related to its weight fraction $x_\text{fm,p}$ through [5]

$$\omega_\text{fm,p} = \frac{x_\text{fm,p}}{x_\text{fm,p} + (1 - x_\text{fm,p})\rho_\text{fm,p}/\rho_\text{pol,p}}, \tag{20}$$

where $\rho_\text{fm,p}$ is the density of the ferromagnetic material in the magnetic drug
carrier particle and $\rho_\text{pol,p}$ is the density of the polymer material in the magnetic
drug carrier particle.

Finally, the particle trajectories are obtained from evaluating the streamline
function

$$\frac{\partial\psi}{\partial y} = -v_{\text{p},x}, \tag{21}$$

$$\frac{\partial \psi}{\partial x} = -v_{p,y}, \tag{22}$$

where ψ is the stream function, and $v_{p,x}$ and $v_{p,y}$ are the components of $\vec{v}_p$ which are given by Eq. (16). The system performance of this model is calculated in terms of the capture cross section, λ_c, defined as

$$\lambda_c = \frac{y_c}{R_{seed}}, \tag{23}$$

where y_c is the capture radius of the ferromagnetic seed. The capture radius, y_c, is defined by the location of the streamline at the entrance to the CV of the last magnetic drug carrier particle captured to the seed. All calculations were performed using the open-source software finite volume library Open-FOAM [13].

6 Results and Discussions

In this simulation iron is used as the magnetic drug carrier particle and SS 409 is used as the seed ferromagnetic material. The streamline functions for the capture of nanoparticles are presented in Fig. 2 for particle radius $R_p = 50\,\text{nm}$, containing $40\,\text{wt}\%$ iron ($x_{fm,p} = 0.4$), under the influence of homogenous magnetic field $\mu_0 H_0$ oriented perpendicularly to the flow ($\theta = \pi/2$) with magnitudes of 0.0 to 0.6 T. In this a single SS409 ferromagnetic seed, with $1\,\mu\text{m}$ radius is located in the CV. The resulting capture cross-section, λ_c, is calculated and presented in Fig. 3 for $50\,\text{nm}$ particles, as a function of the magnetic field strength $\mu_0 H_0$. In the model the magnetisation of the individual nanoparticles is taken as the average value given by the Langevin function. The values of the capture cross-section predicted through use of the Langevin function

(a) $\mu_0 H_0 = 0.0$ T (b) $\mu_0 H_0 = 0.2$ T

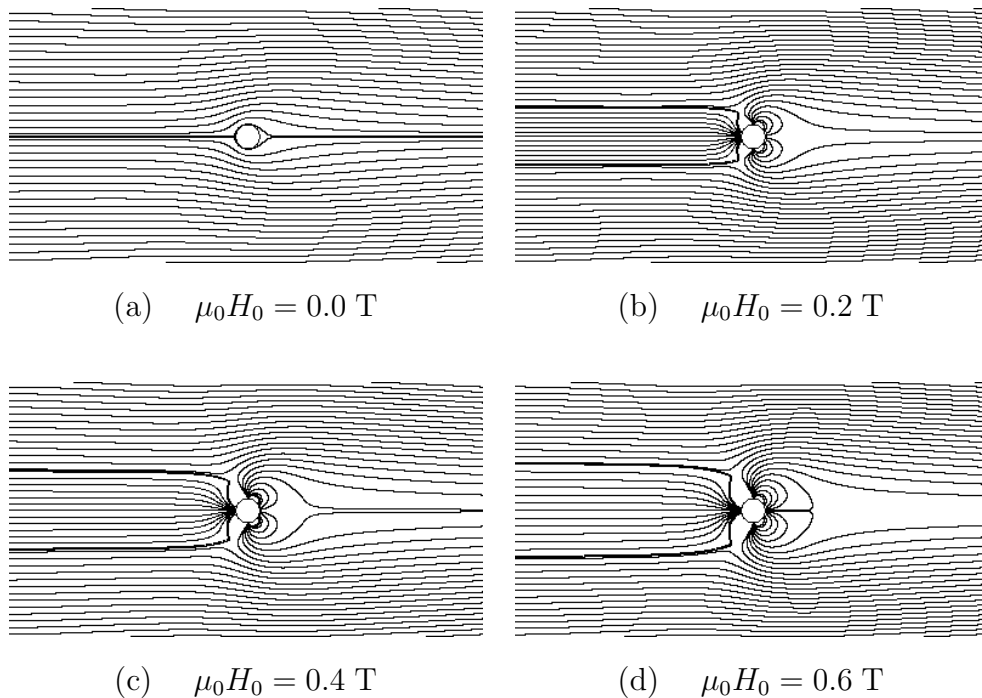(c) $\mu_0 H_0 = 0.4$ T (d) $\mu_0 H_0 = 0.6$ T

Fig. 2. Streamlines indicating the trajectories of the single domain nanoparticles, calculated using OpenFOAM, as they traverse the control volume for different magnitudes of the externally applied magnetic field, $\vec{H}_0$.

135 are significantly larger (see Fig. 3) than would result from the large parti-
136 cle approach taken by Avilés *et al.*. Beyond a field of ≈ 0.7 T, for the material
137 used in this simulation, the carrier particle magnetisation is saturated for both
138 models, leading to identical results.

139 In order to calculate the blood velocity an uniform inlet velocity of 0.1 cm/s
140 is applied to the model. Other important system and parameters of the fer-
141 romagnetic materials that are used in the magnetic drug carrier particles and
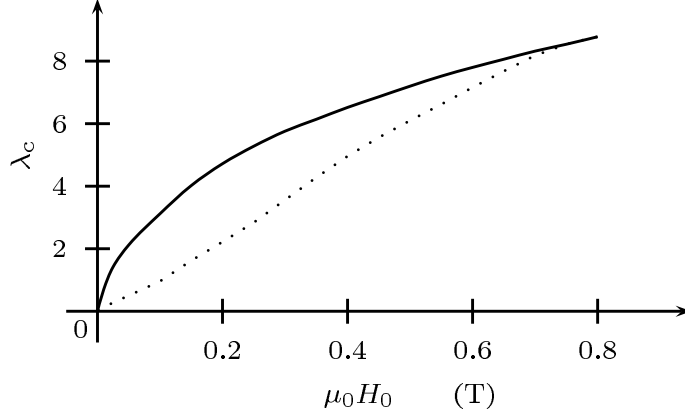142 for the seeds are given in Table 1.

Fig. 3. Capture cross section, λ_c, plotted as a function of the applied magnetic field strength, $\mu_0 H_0$, calculated using (——) the Langevin function as appropriate for single domain particles and (·····) without Langevin function as appropriate for multiple domain particles.

Property	Value	SI Unit	Property	Value	SI Unit
ρ_b	1 040.0	$\mathrm{kg\,m^{-3}}$	$\chi_{\mathrm{seed},0}$	1 000	
η_b	0.002	$\mathrm{kg\,m^{-1}\,s^{-1}}$	$M_{\mathrm{seed,s}}$	1 397 000	$\mathrm{A\,m^{-1}}$
u_0	0.001	$\mathrm{m\,s^{-1}}$	$M_{\mathrm{fm,p,0,s}}$	1 735 000	$\mathrm{A\,m^{-1}}$
$\mu_0 H_0$	0.0–0.8	$\mathrm{kg\,s^{-2}\,A^{-1}}$	R_s	1.0×10^{-6}	m
$x_{\mathrm{fm,p}}$	0		R_p	50×10^{-9}	m
$\rho_{\mathrm{fm,p}}$	7 850	$\mathrm{kg\,m^{-3}}$	$\rho_{\mathrm{pol,p}}$	950	$\mathrm{kg\,m^{-3}}$
$\chi_{\mathrm{fm,p},0}$	1 000				

Table 1

Values of system and material parameters used in the simulation.

143 ## 7 Conclusions

144 The model of Avilés, Ebner and Ritter has been considered for collecting

145 single domain magnetic drug carrier nanoparticles. Here the Langevin function

10

is used to calculate the expected value of the nanoparticle magnetisation. Magnetic flux density $\vec{B}$ is calculated analytically by using the separation of variable solution and the blood velocity $\vec{v}_{\mathrm{b}}$ is obtained from the Navier-Stokes equation using the finite volume library OpenFOAM. The simulations indicate that use of the Langevin function predicts greater collection efficiency than might be otherwise expected.

8   Acknowledgements

References

[1]   Q. A. Pankhurst, J. Connolly, S. K. Jones, J. Dobson, Applications of magnetic nanoparticles in biomedicine, J. Phys. D: Appl. Phys. 36 (2003) R167–R181.

[2]   C. C. Berry, A. S. G. Curtis, Functionalisation of magnetic nanoparticles for applications in biomedicine, J. Phys. D: Appl. Phys. 36 (2003) R198–R206.

[3] A. D. Grief, G. Richardson, Mathematical modelling of magnetically targeted drug delivery, J. Magn Magn Mater. 293 (1) (2005) 455–463.

[4] G. Iacob, O. Rotariu, N. J. C. Strachan, U. O. Häfeli, Magnetizable needles and wires - modeling an efficient way to target magnetic microspheres in vivo, Biorheology 41 (2004) 599–612.

[5] J. A. Ritter, A. D. Ebner, K. D. Daniel, K. L. Stewart, Application of high gradient magnetic separation principles to magnetic drug targeting, J. Magn Magn Mater. 280 (2-3) (2004) 184–201.

[6] M. O. Avilés, A. D. Ebner, H. Chen, A. J. Rosengart, M. D. Kaminski, J. A. Ritter, Theoretical analysis of a transdermal ferromagnetic implant for retention of magnetic drug carrier particles, J. Magn Magn Mater. 293 (1) (2005) 605–615.

[7] H. Chen, A. D. Ebner, M. D. Kaminski, A. J. Rosengart, J. A. Ritter, Analysis of magnetic drug carrier particle capture by a magnetizable intravascular stent: Parametric study with multi-wire two-dimensional model, J. Magn Magn Mater. 293 (1) (2005) 616–632.

[8] B. B. Yellen, Z. G. Forbes, D. S. Halverson, G. Fridman, K. A. Barbee, M. Chorny, R. Levy, G. Friedman, Targeted drug delivery to magnetic implants for therapeutic applications, J. Magn Magn Mater. 293 (1) (2005) 647–654.

[9] E. J. Furlani, E. P. Furlani, A model for predicting magnetic targeting of multifunctional particles in the microvasculature, J. Magn Magn Mater. 312 (1) (2007) 187–193.

[10] M. O. Avilés, A. D. Ebner, J. A. Ritter, Ferromagnetic seeding for the magnetic targeting of drugs and radiation in capillary beds, J. Magn Magn Mater. 310 (1) (2007) 131–144.

12

194 [11] M. I. Shliomis, Magnetic fluids, Sov. Phys. Usp. 17 (3) (1974) 153–169.

195 [12] H. C. Bryant, D. A. Sergatskov, D. Lovato, N. L. Adolphi, R. S. Larson,

196   E. R. Flynn, Magnetic needles and superparamagnetic cells, Phys. Med.

197   Biol. 52 (14) (2007) 4009–4025.

198 [13] OpenCFD Ltd, OpenFOAM 1.4, http://www.opencfd.co.uk (2007).